Bull. Chem. Soc. Ethiop. **2026**, 40(10), 2157-2171.
DOI: https://dx.doi.org/10.4314/bcse.v40i10.8

ISSN 1011-3924
Printed in Ethiopia
Online ISSN 1726-801X

SYNTHESIS, CHARACTERIZATION, AND EVALUATION OF ZEOLITE MATERIAL FOR THE REMOVAL OF CHROMIUM (Cr^{3+}) FROM CONTAMINATED WATER

Umudi Ese[1], Idiege Kimson[2], Erienu Obruche[3], Apuyor Stanley[4], Ekanem Ese[5], Njor Oru Ogar[6], Edidiong Ikpe[7], Abdul Ganiwu Mohammed[8], Clark Poro[9], Ikechukwu Chikwe[10] and Onwugbuta Godpower[11]

[1]Department of Chemistry, University of Agbor, Delta State
[2]Department of Science Education, University of Calabar, CRS, Nigeria
[3]Department of Chemistry, Delta State College of Education, Mosogar, Nigeria
[4]Department of Industrial Chemistry, Dennis Osadebay University, Asaba, Nigeria
[5]Department of Environmental Resources Management, University of Calabar, Nigeria
[6]Department of Science Laboratory Technology, Federal Polytechnic, Ugep. Nigeria
[7]Department of Chemistry, Akwa Ibom State University, Nigeria
[8]Department of Applied Chemistry, University of Technology and Applied Sciences, Ghana
[9]Department of Chemistry, Federal University of Petroleum Resources, Effurun, Nigeria
[10]Department of Science Laboratory Technology, Imo State Polytechnic, Omuma. Nigeria
[11]Department of Biochemistry/Chemistry Technology, University of Port Harcourt, Nigeria

(Received September 3, 2025; Revised on January 4, 2026; Accepted June 22, 2026)

ABSTRACT. Zeolite crystals were synthesized by combining sodium silicate and sodium aluminate to form an aluminosilicate gel, which was then hydrothermally treated to produce the final product. The zeolite crystals were analyzed using X-ray diffraction (XRD), Scanning electron microscopy (SEM), Energy dispersive x-ray diffraction (EDX), and Fourier Transform Infrared (FTIR) Spectroscopic Analysis. Batch adsorption tests and the atomic absorption spectroscopy with the synthetic zeolite demonstrated effective removal of chromium(III) ions from the contaminated water. During the treatment, various amounts of zeolite from 0.5 to 2.5 g were utilized, along with different concentrations of Cr(III) ions (10, 15, 20, 25, 30 ppm). The percentage of adsorption rose from 55.75 to 96.6% and fell from 98 to 88.3% in each of the stages. As the pH levels were adjusted between 1 and 11, the percentage of adsorption increased from 55 to 97%, with a significant rise at pH 7. The high percentage of adsorption in the zeolite samples indicates that zeolites are effective adsorbents for removing Cr from aqueous solutions. Additionally, the batch experiment revealed that the adsorption pattern conformed to the Langmuir and the Freundlich isotherm models, with correlation factors (R2) of 0.997 and 0.963, respectively.

KEY WORDS: Zeolite, Heavy metal, Chromium, Adsorption, Solution

INTRODUCTION

Water contamination is a significant environmental issue that affects both human health and ecosystems [1]. Industrial activities, including mining, electroplating, and tannery operations, often release a variety of toxic pollutants into aquatic environments [2]. Among these, heavy metals such as chromium are of particular concern due to their toxic, carcinogenic, and non-biodegradable nature [3,4]. Chromium exists in two main oxidation states in environmental settings: chromium (Cr^{3+}) and chromium(Cr^{6+}). While Cr(VI) is highly toxic, carcinogenic, and mobile in the environment, Cr(III) is generally considered less hazardous due to its relatively low toxicity and reduced mobility [5-7]. However, elevated concentrations of Cr(III) in water still

*Corresponding author. E-mail: kenkennedy767@gmail.com

pose risks to aquatic organisms and can affect the overall quality of drinking water [8,9]. Therefore, the removal of Cr(III) ions from contaminated water sources is crucial for environmental and public health protection [10-12]. To mitigate the impact of chromium ions in contaminated water, various techniques have been developed, including chemical precipitation, ion exchange, membrane filtration, and adsorption [13-15]. Among these, adsorption is considered one of the most effective, economical, and sustainable methods due to its simplicity, cost-effectiveness, and ability to remove pollutants to very low concentrations [16-18]. Zeolites, a class of crystalline aluminosilicate minerals, have gained considerable attention as potential adsorbents due to their high surface area, porous structure, and ion-exchange properties [19]. They are naturally occurring and can also be synthesized, offering a versatile material for water treatment applications [20, 21]. The specific properties of zeolites, such as their pore size, ion-exchange capacity, and stability under various environmental conditions, make them an ideal candidate for removing heavy metals like chromium, especially Cr(III), which can be adsorbed via ion-exchange and surface interactions [22]. Zeolites can be synthesized by various methods, including hydrothermal synthesis, sol-gel processes, and the use of templates [23]. The synthetic approach and the conditions under which zeolites are prepared influence their structure, surface properties, and overall efficiency in ion removal [24]. Furthermore, modifying zeolite frameworks by incorporating different elements or functional groups can enhance their adsorption capacity and selectivity for specific contaminants, such as chromium ions [25-27].

While there has been significant research on the use of zeolites for removing heavy metals from water, including chromium, several gaps in knowledge remain that hinder the widespread application of these materials [28-30]. These gaps include: (i) Limited Focus on Cr(III) vs. Cr(VI) Removal: Most of the research on zeolite-based adsorbents has concentrated on Cr(VI) removal, given its higher toxicity and greater mobility in aquatic environments. Cr(VI) is soluble in water and readily migrates, making it a more pressing concern for water treatment. However, Cr(III) also poses environmental risks and is often found in water sources in substantial concentrations, particularly from industrial processes like metal finishing and leather tanning [31-33]. Despite this, the majority of studies on zeolite adsorption have focused more on Cr(VI), and less attention has been given to the specific mechanisms involved in the adsorption of Cr(III). This gap in research on Cr(III) removal limits our understanding of how zeolites can be optimized for this particular metal ion [34]. (ii) Performance at High Chromium Concentrations: Another important gap in the research is the limited exploration of zeolite performance at high chromium concentrations, which are typically encountered in natural water bodies. Most laboratory studies use low concentrations of chromium to test zeolite efficiency, but in real-world applications, chromium levels in some water are often much higher. As a result, zeolite materials that work well at low concentrations may not be effective at high concentrations, which are more typical of contaminated water sources [35, 36]. This gap in research underscores the need for more realistic testing conditions that mimic actual environmental scenarios.

This research focuses on the synthesis and characterization of zeolites for the removal of chromium (III) ions from water. The study aims to investigate the adsorption properties of synthesized zeolites, including their efficiency and capacity involved in chromium (III) removal. Additionally, the work explores various characterization techniques to analyze the physicochemical properties of the zeolites, including X-ray diffraction (XRD), scanning electron microscopy (SEM), Energy dispersive X-ray Diffraction (EDX) and Fourier Transform Infrared (FTIR) Spectroscopic Analysis. By understanding the structure and behavior of zeolites, the study seeks to develop a more efficient and sustainable method for removing chromium (III) from contaminated water sources [37, 38]. Through this investigation, the potential of zeolites as an eco-friendly and efficient material for environmental remediation can be better understood, contributing to the development of cost-effective water treatment solutions for the removal of toxic chromium(III) [39, 40].

EXPERIMENTAL

All reagents and chemicals utilized were of commercial (analytical) grade and were employed as received without any additional purification unless stated otherwise. Sodium metasilicate (99.99 % purity), Sodium hydroxide (90% purity), Aluminum hydroxide (64.5% purity), all from Sigma Aldrich, Potassium hydroxide (90% purity) (Qualikems), and Chromium nitrate salt (99% purity) (M and B England) were used, while distilled water was sourced from the Department of Physics, University of Nigeria, Nsukka.

Methods for the synthesis of zeolites

The synthesis method employed was based on the procedure outlined by [41], with certain modifications, that is, by using a different molar ratio of sodium silicate and sodium aluminate. Zeolite crystals were produced through a hydrothermal process (where crystallization occurred in an aqueous environment containing the requisite reactants at elevated temperatures) with slight alterations (by using a temperature of 180 °C and a Pressure of 2 atm) as previously documented of temperature of 150 °C and a Pressure of 3 atm by [41]. The design of the experiment involves: Preparation of the Gel, addition of alkaline solution, addition of water, addition of structure-directing agent, hydrothermal crystallization, Cooling and Filtration, Washing and purification, and finally drying of the zeolite. The synthesis of zeolite can be summarized with two phases: the first phase involves the formation of sodium silicate, while the second phase pertains to the creation of the initial gel. Both reactions are represented by the following chemical equations;

Formation of sodium aluminate

$$2NaOH + Al_2O_3 + 3H_2O \longrightarrow \underset{\text{Sodium aluminate}}{2NaAlO_2} + 4H_2O$$

Starting gel formation

$$\underset{\text{Sodium silicate}}{Na_4SiO_4} + \underset{\text{Sodium aluminate}}{2NaAlO_2} + H_2O \longrightarrow \underset{\text{Starting gel}}{2Na_2O.Al_2O_3.1.75SiO_2.7H_2O}$$

Preparation of starting gel

To make the synthesis gel, 10 g of sodium hydroxide was mixed with 10 g of water while stirring continuously until it fully dissolved. Then, 9.75 g of aluminum hydroxide was measured and added to the clear mixture, which was heated at 100 °C for 3 hours to create a uniform mixture. After that, the mixture was cooled to 25 °C and combined with 20.25 g of distilled water. This mixture was labeled as solution A. Next, 10 g of solution A was combined with 6.12 g of water and 5.91 g of sodium hydroxide, stirring until everything dissolved. Solution B was created by mixing 21.97 g of sodium silicate solution, 61.20 g of water, and 5.91 g of sodium hydroxide until fully dissolved. Solutions A and B were then quickly mixed together while stirring vigorously for 3 hours, resulting in an opaque gel.

Gelation and aging

After mixing the ingredients, that is, solution A and B, the gel was allowed to age at room temperature for 8 hours so that it could give the desired characteristics of the zeolite we want. Aging was carried out to ensure the development of the initial gel structure, which is important for crystallization. The aging of the gel was also carried out to stabilize the gel before it undergoes crystallization.

Crystallization

The resulting homogeneous opaque gel after aging was the final product before crystallization. This gel was placed into a Cylindrical Polytetrafluoroethylene [PTFE] vessel, which was then put inside a sealed PTFE pressure vessel. The vessel was placed in an oven at 180 °C and 2 atm for 8 hours to allow crystallization to occur without stirring. This process is done under these high temperature and pressure conditions to promote the crystallization of the zeolite structure we desired.

Product recovery

Cooling and filtration

After the crystallization period, the Cylindrical Polytetrafluoroethylene [PTFE] vessel was cooled in ice water for 30 minutes before being opened. After cooling, the zeolite crystals are recovered by filtration to separate them from the remaining liquid phase.

Washing and purification

The zeolite crystals are washed several times with deionized water to remove any residual alkali, organic template, or unreacted starting materials and centrifuged. This process was repeated until the supernatant solution reached a pH of 7. The washing process is essential to remove any impurities and ensure the purity of the final product.

Drying and activation

After washing and template removal, the zeolite was dried in an oven at around 100 °C for 6 hours to remove any remaining water. After drying, further thermal treatment was done to activate the zeolite, making it more effective for its use as an adsorbent. This was done by heating the zeolite to temperatures of from 200 °C to be suitable for the intended use of removing chromium (iii) ions from water.

Batch adsorption studies

Adsorption experiments were conducted using synthesized zeolite particles in glass beakers. To find out how much chromium metal can be absorbed by the zeolite, a stock solution of Cr^{3+} at 1000 mg/L was made by dissolving 6.67 g of $Cr(NO_3)_3.9H_2O$ in distilled water and filling it up to the mark in a 1000 mL volumetric flask. A series of tests was done to observe how zeolite adsorbs Cr^{3+} ions. In each test, 50 mL of the Cr^{3+} solution was added to 100 mL vessels to keep the concentration and volume consistent.

Effect of metal ion concentration

To examine the impact of metal ion concentration, the zeolite mass was kept constant at 2 g for 50 mL of Cr^{3+} solution across various Cr^{3+} concentrations (10, 15, 20, 25, 30 ppm). Exactly 2 g of the zeolite sample was placed in 100 mL vessels with different Cr^{3+} ion concentrations. The mixture was stirred using a multifix mixer for 1 hour. After stirring, the mixture was filtered, and the filtrate was analyzed using Atomic Absorption Spectroscopy (AAS).

Effect of adsorbent dosage

The influence of adsorbent quantity was studied by keeping the Cr^{3+} concentration constant at 20 ppm while varying the mass of the zeolite samples (0.5 g, 1.0 g, 1.5 g, 2.0 g, 2.5 g). Different amounts of zeolite were mixed with 50 mL of the 20 ppm Cr^{3+} solution. The mixture was stirred for 1 hour and then filtered. The resulting filtrates were analyzed using AAS.

Impact of pH on the adsorption rate

This research examined how pH affects the adsorption of Cr^{3+} ions on zeolite particles across a pH range of 1.0 to 11.0, using a constant zeolite dosage of 2 g and a Cr^{3+} concentration of 20 ppm at room temperature. The pH was adjusted with 0.5 M HNO_3 or 0.5 M NaOH solutions (before adding the adsorbent) while shaking continuously for 1 hour. The final ion concentration in the filtrate was measured using AAS.

Effect of varying particle sizes

To assess the impact of different particle sizes on the adsorption rates of various synthesized samples, 2 g of each zeolite sample (with distinct particle sizes) was measured into separate reaction vessels containing 20 ppm concentrations of the Cr^{3+} solution. The mixtures were subsequently stirred using a multifix mixer for 1 hour at ambient temperature. Following this, the suspensions were filtered using a centrifuge, and the resulting filtrate samples were examined for ion concentration through atomic absorption spectroscopy (AAS).

Statistical analysis

Descriptive statistics were used to determine the average adsorption at each concentration, along with standard deviation, to provide insight into the central tendency and spread of the data. A linear regression statistics model was also used to quantify the relationship between Cr^{3+} concentration and adsorption, as shown in Figures 5A and 5B. This approach ensures that the observed effects were not due to random chance but provides a clear mathematical model for predicting adsorption behavior at various Cr^{3+} concentrations.

RESULTS AND DISCUSSION

Characterization before adsorption

To begin any synthesis process, it is essential to understand the composition or structure of the final product. After synthesizing zeolite, it is important to clarify its physical morphology and chemical components. The final products were characterized using SEM and XRD, which provide useful insights into the chemistry of the zeolite, helping to determine if zeolite was successfully produced through this method [42].

Scanning electron microscopy (SEM) and X-ray diffraction (XRD)

Scanning electron microscopy **(**SEM) is a specialized tool that captures images of a sample by scanning its surface with a focused electron beam. This interaction generates various signals that create micrographs, offering valuable information about the sample's composition and surface topography. Figure 1 B and C shows the SEM micrographs of the zeolite. The main goal of SEM is to display the surface structure and actual morphology of the zeolite, which has a rough and irregular shape, porosity, and a compact structure. These SEM images clearly demonstrate that

the particles are disc-shaped, with sizes ranging from 13.4 to 54.0 µm. The differences in the sizes of the synthesized zeolite particles resulted from carefully adjusting the size and shape of the zeolite samples produced. The growth in particle sizes, as indicated by these SEM images, can be linked to the increased volume of water used in preparing the initial gel. A similar perspective was expressed by [43] regarding the synthesis of nanoporous zeolite [44].

The X-ray diffraction (XRD) method is widely used to assess the crystallinity and noncrystallinity of materials through their diffraction peaks. By analyzing these specific peaks, including their sharpness, quantity, intensity, positions, and spacing, one can evaluate the crystallinity of the synthesized nanoparticles. Crystalline substances usually display clear, sharp peaks with several distinct peaks and high intensity, indicating a greater degree of crystallinity. On the other hand, amorphous materials with lower crystallinity may show broad or diffuse peaks with reduced intensity. Figure 1A illustrates the XRD spectrum featuring diffraction peaks for zeolite. The diffraction positions align well with the JCPDS44-0141 file. Based on the pattern obtained, faujasite zeolite was identified through the XRD results. The characterization of the XRD pattern revealed a single phase of faujasite zeolite. This finding is consistent with previous research by [21].

A

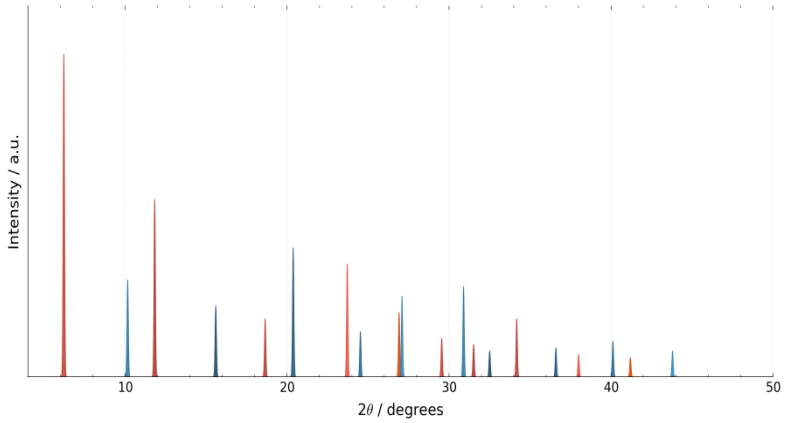

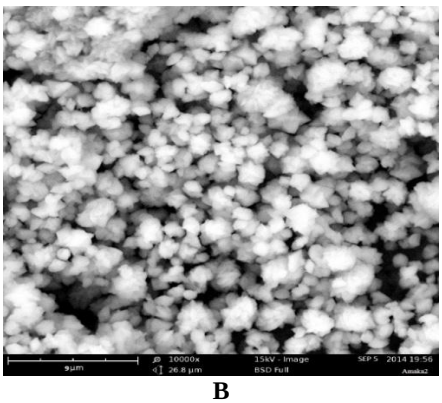

B

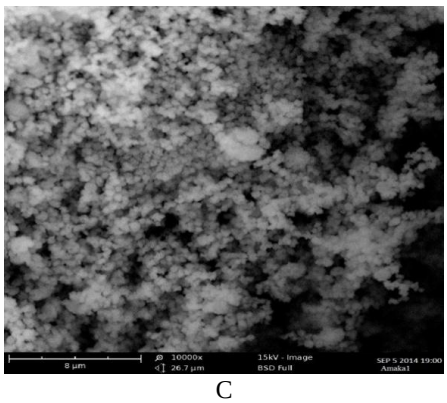

C

Figure 1. Imaging characterization of synthesized zeolites **(**A**),** XRD (B and C), various morphologies of SEM images.

The energy-dispersive X-ray (EDX)

The Energy Dispersive X-ray Diffraction (EDX) analysis is a key instrumental method that identifies the elemental components present in materials based on their weight percentages. When an element is stimulated by an external source, typically an electron beam in an electron microscope, it emits characteristic X-rays that are captured by the instrument. The energy-dispersive X-ray (EDX) spectra illustrated in Figure 2 indicate that the zeolite's composition comprises three primary elements: silicon, aluminum, and sodium, along with trace amounts of potassium, magnesium, iron, and calcium. The chemical compositions (weight percent) of the zeolite are presented in Figure 2. The zeolite spectra reveal optical absorption values as follows: SiO_2 at 70.3% (w/w), Al_2O_3 at 17.7% (w/w), Na_2O at 5% (w/w), K_2O at 1.4% (w/w), MgO at 0.75% (w/w), Fe_2O_3 at 0.39% (w/w), and CaO at 0.89% (w/w), respectively. No additional elements were detected as impurities, indicating the successful synthesis of the zeolite. Other elements that appeared, such as iron and calcium, may have originated from the synthesis process or the reagents utilized in the preparation of the zeolite. The energies of these X-rays correspond to specific elements within the sample, facilitating the identification and quantitative analysis of individual components.

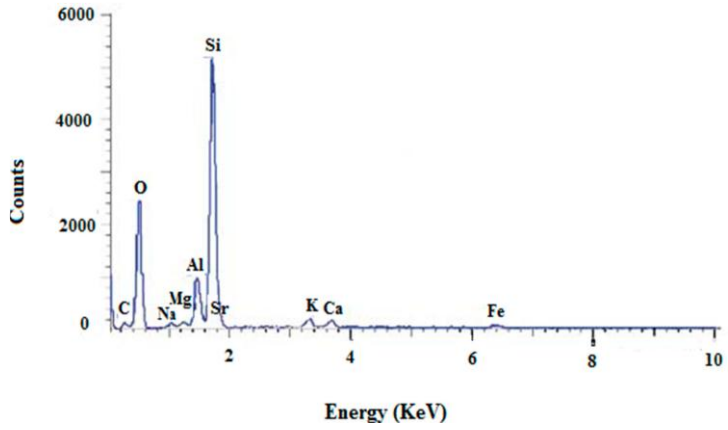

Figure 2. EDX spectrum of synthesized zeolites.

Fourier transform infrared (FTIR) spectroscopic analysis

Figure 3 illustrates the chemical characteristics of the synthesized zeolite, specifically highlighting the functional groups located on its surface. The analysis was conducted using FTIR spectrophotometry with the model Nicolet iS10 FT-IR Spectrometer, operating within a wave number range of approximately 3000 to 763 cm^{-1}. The prominent bands of the aluminosilicate were identified within the range of 752–827 cm^{-1}. These absorption bands correspond to the asymmetric stretching of Si–O–Si and the stretching vibrations of Si–O–Al, which were noted at 1006.4 and 1118.2 cm^{-1}, respectively [45]. Additionally, peaks observed at 1565–1371 cm^{-1} and around 3000 cm^{-1} delineate the presence of two distinct groups of bands. The first group is associated with the bending vibrations of H_2O molecules that are adsorbed on the zeolite's surface, while the second group, characterized by a broad band near 3000 cm^{-1}, signifies the elongation vibrations of the OH groups from the water molecules within the zeolite [45].

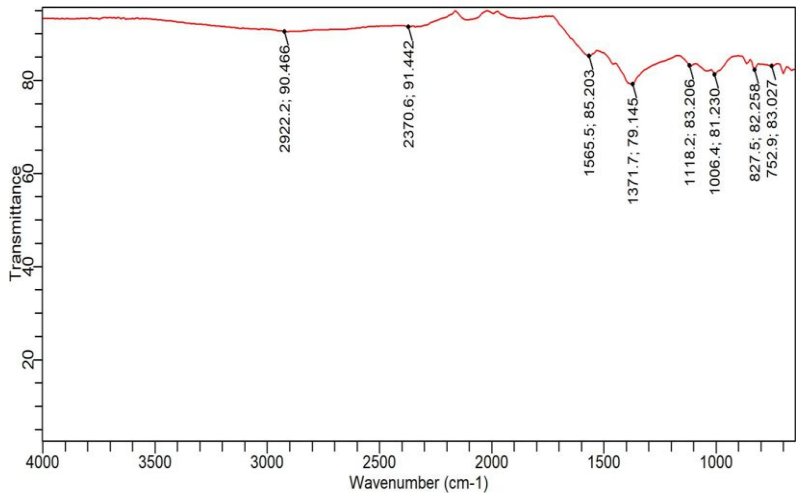

Figure 3. FTIR Spectral for the synthesize zeolite.

Characterization after adsorption

The energy-dispersive X-ray (EDX) and scanning electron microscopy (SEM)

For the energy-dispersive X-ray (EDX), after the adsorption of chromium(III) ions, the EDX spectrum of the zeolite clearly displays the characteristic peaks for chromium, typically around 4.8 keV (Kα). The presence of these peaks, alongside the stable peaks for silicon and aluminum, provides direct evidence of the zeolite's ability to adsorb chromium from water, as shown in Figure 4b. The intensity of the chromium peaks showed the amount of chromium adsorbed and also quantifies the adsorption process; while minor, the shifts in the silicon and aluminum peaks suggest subtle changes in the zeolite's structure or chemistry. Thus, this characterizes EDX analysis after the sorption as a powerful tool for monitoring the effectiveness of chromium removal and understanding the underlying interactions between the metal ions and the zeolite structure.

For the scanning electron microscopy (SEM), after chromium (III) ion adsorption, the SEM characterization of the zeolite showed significant changes in surface morphology, including roughening of the surface, particle aggregation, possible surface deposits, and alterations to the pore structure, as shown in Figure 4a. These visual alterations are indicative of the zeolite's interaction with the chromium ions, reflecting its adsorption capacity and providing insights into the efficiency and mechanism of chromium removal from water. Additionally, the presence of chromium species or oxide phases in the EDX further confirms the ion-exchange and adsorption processes.

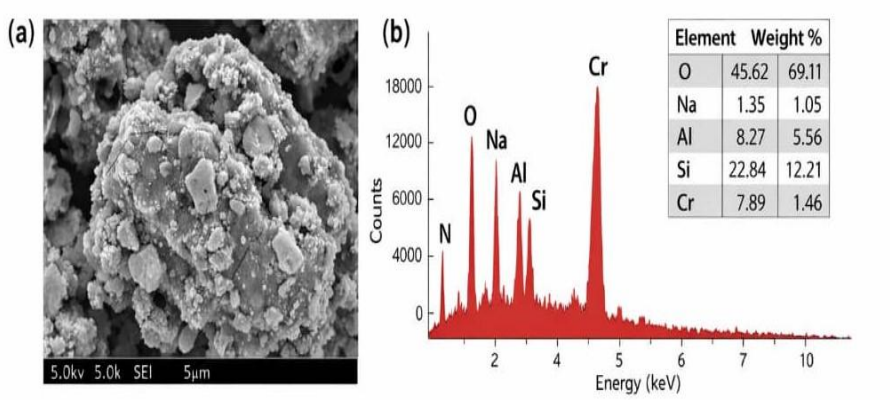

Figure 4. (a) SEM Image of the zeolite after adsorption, (b) EDX spectra of the zeolite after adsorption

Fourier transform infrared (FTIR) spectroscopic analysis

FTIR spectra of the zeolite after Cr(III) adsorption showed noticeable shifts and intensity changes in the O–H stretching and Si–O–Si/Si–O–Al vibration bands, indicating interaction between chromium ions and surface hydroxyl groups. The appearance of weak bands in the 680–520 cm^{-1} region further confirms the formation of Cr–O bonds, suggesting that Cr(III) adsorption occurs mainly via ion exchange and surface complexation mechanisms without significant alteration of the zeolite framework.

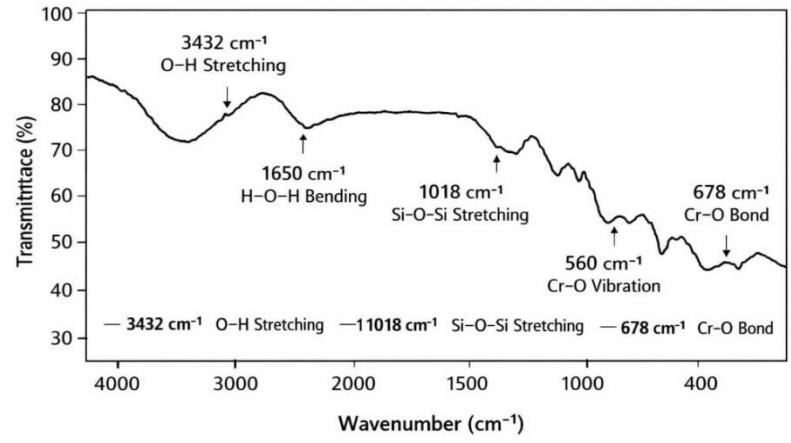

Figure 4. FTIR Spectral after adsorption.

Adsorption of chromium ion

Impact of adsorbent dosage

Table 1 illustrates how zeolite dosage affects the adsorption of Cr^{3+} from water. The percentage removal efficiency rises as the amount of adsorbent increases, as shown in the table. The rise in

adsorption rate with more zeolite may be due to a larger surface area; a greater quantity of adsorbent (zeolite) effectively reduces the saturation of the adsorption sites, leading to a decrease in the number of available sites per unit mass. It was noted that increasing the mass of zeolite enhanced the adsorption rate of metal ions. This can be linked to the increase in surface area per unit volume of solution available for adsorption with the zeolite sample.

Table 1. Shows the effect of the mass of adsorbent at an initial metal ion concentration (Co) of 20 ppm and the concentration of unadsorbed metal ion (C).

Samples	Mass of adsorbent (g)	Concentration(C) (ppm)	Percentage adsorption (%)
1	0.5	8.85	55.75
2	1.0	6.02	69.90
3	1.5	3.98	80.35
4	2.0	0.85	95.75
5	2.5	0.68	96.60

Effect of metal ion Cr^{3+} concentration

The adsorption rate based on metal ion concentration was examined at room temperature with a shaking duration of 1 hour, while the amount of zeolite (the adsorbent) remained constant at 2 grams. The concentration of heavy metal ions varied from 10 ppm to 30 ppm. The results of this experiment are presented in Table 2. Also, from the table, it indicates that the percentage of adsorption decreased as the metal ion concentration increased. The quantity of metal ions adsorbed per unit mass of zeolite (adsorbent) gradually rose with the increase in metal ion concentration; however, the overall extent of adsorption declined with higher metal ion loading. It was noted that at lower metal ion concentrations, the ratio of metal ions to available adsorption sites was low, making the adsorption independent of the initial concentration. As the concentration of metal ions increased, competition for adsorption sites intensified, leading to a unit mass of zeolite being exposed to more metal ions, which gradually occupied the binding sites.

Table 2. Effect of metal ion concentration at initial concentration (C_o), concentration of unabsorbed metal ion (C) and mass of adsorbent, 2.0 g.

Samples	C_o (ppm)	C (ppm)	Percentage adsorption (%)
1	10	0.20	98.0
2	15	0.45	97.0
3	20	0.83	95.9
4	25	1.95	92.2
5	30	3.50	88.3

Effect of pH

Table 3 presents data on how pH affects the adsorption rate of Cr^{3+} on zeolite particles. From the table, it is evident that as pH rises, the percentage of adsorption also increases, peaking at pH 7, where there is a significant jump in percentage adsorption. This increase continues at a slower rate as pH rises from 9 to 11. This pattern may occur because, at lower pH levels, H_3O^+ ions outnumber Cr^{3+} ions, making it difficult for Cr^{3+} ions to compete for binding sites on the zeolite. However, as pH increases, the concentration of H_3O^+ ions drops, providing more binding sites for Cr^{3+} ions.

Table 3. Effect of pH on adsorption rate.

pH	Percentage adsorption (%)
1	55
3	68
5	71
7	93
9	95
11	97

Effect of varying particle sizes

The scanning electron microscopy (SEM) images in Figures 1 clearly indicate that the synthesized zeolite samples have varying pore diameters between 13.4 and 53.6 µm. The adsorption rate related to the sizes of the zeolite particles was examined at room temperature, with a shaking duration of 1 hour, using 2 grams of zeolite and a heavy metal concentration of 20 ppm. The findings of this experiment are presented in Table 4. The results clearly demonstrate that as the water content of the initial gel increased, the particle size of the synthesized zeolite particles also increased progressively. Table 4 illustrates that as the sizes of the synthesized zeolite particles grew, the percentage of adsorption decreased. This may be due to the fact that larger particle sizes diminish the surface area of the zeolite particles, resulting in fewer adsorption sites; conversely, smaller zeolite particle sizes offer a greater surface area for metal ion attachment.

Table 4. Effect of particle size on adsorption rate.

Samples	Particle Size (µm)	C (ppm)	Percentage adsorption (%)
A	13.4	0.22	98.9
B	13.6	0.38	98.1
C	26.4	1.52	92.4
D	26.7	1.50	92.5
E	27.0	1.81	91.0
F	43.8	3.63	81.9
G	46.5	3.90	80.5
H	53.6	5.31	73.5
I	53.7	5.90	70.5
J	54.0	6.01	70.0

Adsorption isotherms

The adsorption study was confirmed using two types of adsorption isotherms: Langmuir and Freundlich. For initial metal concentrations of 10, 15, 20, 25, and 30 ppm, with a constant amount of adsorbent (2 g), the linear forms of the Langmuir and the Freundlich isotherms, based on equations 1 and 2, regarding Cr^{3+} ion removal by zeolite, are illustrated in Figures 5A and 5B, respectively. Both isotherms fit the experimental data well, but the Langmuir model fit better, achieving a correlation factor (R^2) of 0.997, which surpasses the Freundlich correlation factor (R2) of 0.963. A high Q max value indicates a significant uptake of Cr^{3+} ions by the zeolite particles. Adsorption isotherm constants of the adsorption of Cr^{3+} by zeolite are: Q_{max} (Langmuir) is 100, K_L (Langmuir) is 0.001, K_F(Freundlich) is 0.163, and n (Freundlich) is 2.9, respectively.

A

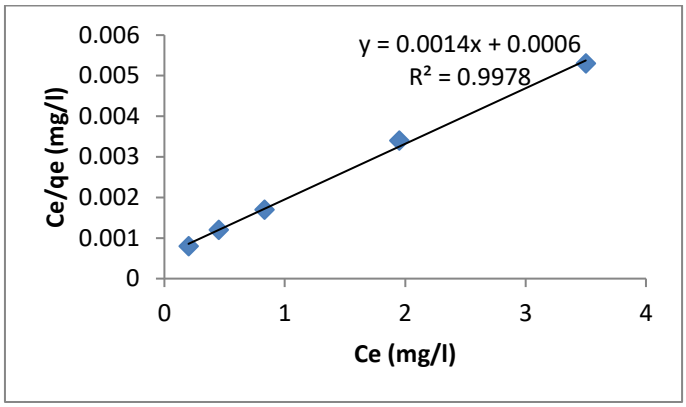

B

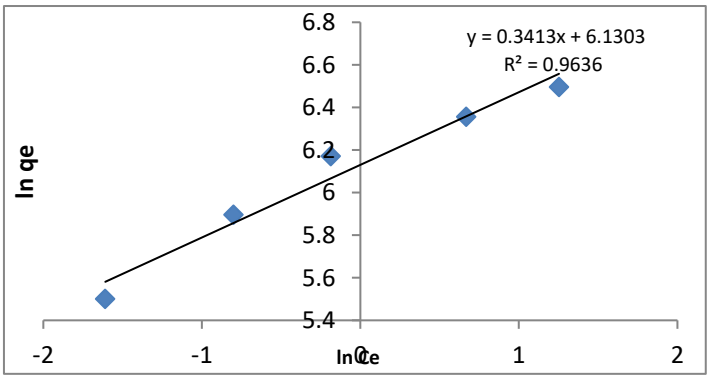

Figure 5. (**A**)Linear Langmuir isotherm plot for the removal of Cr^{3+} by zeolite (**A**) Linear Freundlich isotherm plot for Cr^{3+} removal by zeolite.

CONCLUSION

In this research, zeolite particles were created in the lab using a hydrothermal method with sodium hydroxide and sodium metasilicate. The composition of the starting gel materials was adjusted to produce zeolites of various particle sizes. The zeolite particles were analyzed using XRD and SEM. The synthesized zeolite particles were then tested in adsorption studies with different factors: adsorbent dosage, initial metal ion concentration, pH, and varying particle sizes. It was observed that the percentage of adsorption increased as pH, particle size, and initial Cr^{3+} ion concentration decreased. Additionally, increasing the adsorbent dosage led to a rise in percentage adsorption. The experimental data were evaluated using linear plots of the Langmuir and the Freundlich models, which fit the data well with correlation factor (R^2) values of 0.997 and 0.963, respectively. The Langmuir and the Freundlich models describe the adsorption capability of the adsorbent (zeolite) with a single-layer adsorption, indicating that the adsorption layer is one layer thick. Langmuir supports a scenario where each site has a specific affinity for adsorption, resulting in homogeneous adsorption. Consequently, the Langmuir equation provided a better fit than the Freundlich equation due to its higher correlation factor of 0.997. The findings from this research

indicate that zeolites can effectively sorb chromium metal ions from aqueous solutions. Thus, it can be concluded that zeolites are effective adsorbents for removing chromium ions from aqueous solutions.

REFERENCE

1. Obruche, E.K.; Itodo, A.; Wuana, R.; Sesugh A. Polycyclic aromatic hydrocarbons in harvested rainwater in Warri and Agbarho, Nigeria. *Bull. Chem. Soc. Ethiop*. **2022**, 36, 27-35.
2. Salunkhe, B.; Raut, S.J. Removal of heavy metal Ni(II) and Cr(VI) from aqueous solutions by Scolecite natural zeolite. *Int. J. Chem. Sci.* **2012**, 10, 1134-1143.
3. Dizadji, N.; Seyed, V.S.; Dehpouri, S. Experimental investigation of adsorption of heavy metals (Copper(II)) from Industrial wastewater with synthetic zeolite (4A). *Chem. Trans.* **2012,** 29, 1519-1524.
4. Erdem, E.; Karapina, N.; Donat, R. The removal of heavy metal cations by natural zeolites**.** *J. Colloid Interface Sci.* **2004**, 280, 309-314.
5. Shangying, Q.; Li, H.; Xin, S.; Jin, Y.; Shiqi C.; Yilin, W. FeS_2 nanosheets as mimetic peroxidase for sensitive colorimetric detection of biothiols. *Bull. Chem. Soc. Ethiop.* **2025**, 39, 1699-1711.
6. Michalev, T; Petrov, I. The removal of heavy metals ions by synthetic zeolites. *A Rev. Sc uni. Rousse* **2012**, 5, 1-6.
7. De, V.I.; Beca, C.G. Pine bark for heavy metals removal in waste water treatment. *Euro. Water Pol. Cont.* **1992**, 2, 13-21.
8. Lee, H; Zones, S.I. Davis, M.E. A combustion free methodology for synthesizing zeolite and zeolite-like materials. *Let. Nat.* **2003**, 42, 385-387.
9. Obruche, E. K.; Ogwuche, C.E.; Erhabor, O.D.; Mkurzurum. C .Evaluation of the inhibitive effect of African Marigold (*Tagetes erectal L*.) Flower extracts on the corrosion of aluminium in hydrochloric acid. *Intr. J. Adv. Sc. Res. Engr.* **2019**, 4, 167-177.
10. Silke, M.; Calzaferri, G. Tuning the size and shape of zeolite L- based inorganic-organic host guest composites. *Adv. Funct. Mat.* **2003**, 11, 285-286.
11. Althoff, R; Unger, K.; Schuetto, F. Controlling the spatial; distribution of aluminium in ZSM-5. *Mic. Mat.* **1994**, 2, 557-562.
12. Verduijn, J.P. Chemistry of zeolites and related porous materials.*US Pat.* **1993**, 5, 242-675.
13. Itodo, A.U.; Wuana, R.A; Erhabor, O.D.; Obruche, E.K.; Agbendeh, Z.M. Evaluating the effects of roofing materials on physicochemical properties of harvested rainwater in Warri, Delta state, Nigeria. *Chem. Soc. Niger. J.* **2021**, 12, 234-245.
14. Gure, A.; Chandravanshi, B.S.; Wondimu, T. Metals in green coffee beans from major coffeegrowing regions of Ethiopia. *Chem. Int.* **2014**, 4, 458-468.
15. Kim, G.J.; Ahn, W.S. Direct Synthesis and Characterization of high-SiO_2-content mordenites. *Zeolites* **1991**, 11,745-750.
16. Camblor, M.A; Pe´rez-pariente, J. Crystallization of zeolite beta: Effect of Na and K ions. *Zeolites* **1991**, 11, 202-210.
17. Yonas, B.; Bayetta, B.; Chemeda, F. Evaluation of bean qualities of indigenous Arabica coffee genotypes across different environment. *J. Plant Breed. Crop Sci*. **2014**, 6, 135-143
18. Thompson, R.W.; Huber, M.J. Analysis of the growth of molecular-sieve zeolite NaA in a batch precipitation system. *J. Cryst. Growth* **1982**, 56,711-722.
19. Obruche, E. K; Ogwuche C.E; Erhabor O.D; Mkurzurum. C. Investigating corrosion inhibition effects of *Tagetes Erecta L*. Leaf extract on aluminium in acidic medium. *Glob. Sc. J.* **2019**, 7, 1-17.
20. Onyango, S.; Kuchar, D; Kubota, M.; Matsuda, H. Adsorptive removal of phosphate ions from aqueous solution using synthetic zeolites. *Indust. Engr. Chem. Res.* **2007**, 46, 894-900.

21. Cundy, C.S.; Cox, P.A. Principal proposals for zeolite synthesis. *Micro Meso. Mat.* **2005**, 82, 49-59.
22. Al-Anbera, M.; Zaid A. A. Utilization of natural zeolite as ion exchange and sorbent material in the removal of iron. *Desalination* **2008,** 22, 70-81.
23. Nebesny E.; Budryn, G. Evaluation of sensory attributes of coffee brews from robusta coffee roasted under different conditions. *Eur. Food Res. Technol*. **2006**, 224, 159-165.
24. Obruche, E.K.; Erhabor, O.D; Itodo, A.U; Itopa S.T. Spectrophotometric determination of iron in some commercial iron containinig tablets/capsule. *Int. J. Adv. Trends Comput. Appl.* **2019**, 1, 231-235.
25. Dabrowski, A. Adsorption Form Theory to practice advances in colloid And Interface Science. Adsorption, ion exchange and catalysis. *Indust. Engr. Chem. Res*. **2001**, 93, 135-224.
26. El-Nabarawy, T.H.; Mostafa, R.M.; Youssef, A.M. Activated carbon tailored to remove different pollutants from gas stream and solution. *J. adsr. Sc. and Techn.* **1997**, 3, 15-68.
27. Zamzow, M.J.; Murphy J.E. Removal of metal cations from water using zeolites. *Sep. Sc. Techn*. **1992**, 27, 1969-1984.
28. Ekpo, R.E.; Marcus, A.C.; Obruche, E.K. Spartial and temporal variations in the concentration of particulate matter in ambient air from three different locations in river state, Nigeria. *Int. J. Sci. Res. Chem. Sci.* **2023**, 10, 32-38.
29. Sebastin, P.; Smarshly, B. Nanoporous materials. *J. Nanosci. Nanotechnol.* **2002**, 2, 581-612.
30. Shevade S.; Ford R.G. Use of synthetic zeolites for arsenate removal from pollutant water. *Water Resr*. **2004**, 38, 3197-3204.
31. Wingenfelder, U.; Nowack, B.; Furrer, G. Adsorption of Pb and Cd by amine-modified zeolites. *Water Res.* **2005**, 39, 3287-3297.
32. Ekpo, R.; Obruche, E.K.; Marcus. A. Spatial and temporal variations in the concentrations of polycyclic aromatic hydrocarbon, in ambient air from three different locations in river state, Nigeria. *Intr. J. New Chem.* **2024**, 12, 567-580.
33. Loewenstein, W. A study of Si, Al ordering in thallium zeolite- A by powder neutron diffraction. *Amer. Miner.* **1954**, 39, 92-96.
34. Skoulidas, A.I.; Sholl, D.S. A simulation of hydrogen in metal organic framework. *J. Phy. Chem.* **2002**, 10, 5058-5067.
35. Pearce, M. E.; Mai, H.Q.; Lee, N.; Larsen, S.C.; Salem, A.K. Silicalite nanoparticles that promote transgene expression. *Nanotechnology* **2008**, 19, 1751-1759.
36. Obruche, E.K.; Emakunu, S.O.; Ugochukwu, G.C**.** Rainwater harvesting: Microbial and chemical water quality assessment in Warri district. *Mos. J. of sc. Edu.* **2025**, 10, 36-46
37. Beerdsen, E.; Dubbeldam, D.; Smit, B. Zeolites and catalysis: Synthesis, reactions and applications. *J. Phy. Chem*. **2006**, 3, 22754-22772.
38. Fisher, K.A.; Huddersman, K.D.; Taylor, M.J. Comparism of micro- and mesoporous inorganic materials in the uptake and release of the drug model fluorescein and its analogues. *Chem. Euro. J.* **2003**, 9,5873-5878.
39. John, D. Synthetic zeolites and other microporous oxide molecular sieve. *Resr. Dev. Dept.* **1999**, 96, 3471-3479.
40. Festus-Amadi, I.R.; Erhabor, O.D.; Ogwuche, E.; Obruche E.K. Characterization of contaminated sediments containing polycyclic hydrocarbons from three rivers in the Niger delta region of Nigeria. *Chem. Resr. J.* **2021**, 6, 1-12.
41. Krishna, R.; van Baten, J.M. Separating n-alkane mixtures by exploiting differences in the adsorption capacity within cages of CHA, AFX and ERI zeolites. *Sep. Purif. Technol*. **2008**, 60, 315-320.
42. Paramada, P.N. Sintering behaviour of calcium exchanged ions silica zeolites, synthesized from Kaolin. *Cer. Intr*. **2001**, 21,105-114

43. Ogwuche, C.E; Obruche E.K. Physio-chemical analysis of palm oils (*elaeis guineensis*) obtained from major markets in Agbarho, Unenurhie, Opete, Ughelli and Evwreni town, Delta state, Nigeria. *Intr. J. of trend sc. Res. dev*. **2020**, 4, 56-60.
44. Zang, R.; Li, P.; Guo, X.; Man, Z.; Zhang, S.; Wang, C.; Wang, G. Yolk–shell N-doped carbon coated FeS_2 nanocages as a high-performance anode for sodium-ion batteries. *J. Mater. Chem. A* **2019**, 7, 14051-14059.
45. Mohamed, D.A.; Abdulrahman, A.A; Manar, E.A; Amer A.Z; Omnia,M.H; Ahmed,A.E. Larvicidal and adulticidal effect of green synthesis copper oxide nanoparticles using *Achillea fragrantissima* and its biological and ultra-structural impact on *Culex pipiens*. *Bull. Chem. Soc. Ethiop.* **2025**, 39, 535-546.